Aquaculture Reports 18 (2020) 100451

Contents lists available at ScienceDirect

Aquaculture Reports

journal homepage: www.elsevier.com/locate/aqrep

Effects of tank shapes and aerations on survival, growth and swim bladder inflation of red seabream *Pagrus major* larvae

Aung Naing Win [a], Wataru Yamazaki [b], Tetsuya Sumida [c], Atsushi Hagiwara [a], Yoshitaka Sakakura [a,*]

[a] Graduate School of Fisheries and Environmental Sciences, Nagasaki University, 1-14 Bunkyo-machi, Nagasaki, 852-8521, Japan
[b] Department of Mechanical Engineering, Nagaoka University of Technology, Niigata, 940-2188, Japan
[c] Shipping Technology Department, National Institute of Technology, Oshima College, Yamaguchi, 742-2193, Japan

ARTICLE INFO

Keywords:
Red seabream
Tank shape
Aeration
Survival
Flow field

ABSTRACT

This study aimed to seek for the optimal condition for small-scale larviculture of red seabream *Pagrus major* larvae. We examined the effects of tank shapes and aerations, which were assumed to influence the larval survival, growth and swim bladder inflation of *P. major* larvae. Seawater (50-l) was filled into three cylindrical (CT: 1.7×10^3 cm^2 water surface area, 30 cm deep) and six rectangular (RT: 1.8×10^3 cm^2 water surface area, 28 cm deep) tanks. One air stone with 100 ml/min aeration rate was set at the bottom center of three CT and RT (RT1AS), and two air stones with 50 ml/min aeration rate were set at the half bottom center of three RT (RT2AS). Five hundred eggs were distributed into each experimental tank. Rotifers were fed to larvae at 10 individuals/mL on 3 days post hatching (dph) and their distribution in tanks were measured. Survival rate at 14 dph in CT (54.7 ± 11.0 %) and RT1AS (55.3 ± 6.0 %) were significantly higher than that in RT2AS (29.6 ± 9.3 %, $p < 0.05$). However, the growth of larvae was not significantly different between tank shapes and aerators. Swimbladder inflation rates were not different between tank shapes and aerations, however, CT (58.9±28.3 %) showed lower trend (RT1AS 94.4±6.9 %, RT2AS 92.2±10.7 %). Rotifer distribution in tanks was higher at tank bottom ($p < 0.05$). Low flow regions were observed along the side walls of the tanks and bottom areas in CT and RT1AS due to a single-pair vortex system and formed at the center (between air stones) and from the air stone to the tank walls in RT2AS due to two single-pair vortex systems. These low-flow areas were coincided with higher rotifer distribution areas at the tank bottom indicating that measuring rotifer density can estimate the flow in a tank. We recommend the rectangular tank with one air stone system for red seabream larvae.

1. Introduction

Larviculture experiments are carried out in many different systems from small beakers to very large commercial tanks, and in many cases, variation among the tanks within a given system is high (Kolkovski et al., 2004). This is due to factors such as differences in flow rates, amounts of live and dry food administered, concentration of algae in 'green-water' systems, temperature variation, and lighting (Kolkovski et al., 2004). Therefore, small-scale rearing system is required in order to achieve relevant marine fish larviculture experiments that can easily manipulate the experimental conditions with replicates (Kolkovski et al., 2004; Moorhead, 2015). However, it has been long recognized that better survival and growth of larvae occur in large rearing tanks rather than in smaller systems (Houde, 1972). One reason may be due to the difficulties in manipulating flow field in the small-rearing tanks. Physical parameters such as tank surface area (Ruttanapornvareesakul et al., 2007), tank volume (Theilacker, 1980; Estudillo et al., 1998), and tank shape (Moodie et al., 1992; Moore et al., 1994) can influence water circulation (flow field), larval behavior and ultimately larval growth and survival (Cook et al., 2015). Although tank design is an important basic consideration when culturing marine fish larvae (Tucker, 1998), the importance is not reflected in the literature and a limited number of studies have examined the effects of tank size and shape on marine fish larval growth and survival (Cook et al., 2015). In this study, we aimed to investigate the small-scale marine fish larviculture with commercially available tanks (50 l) with different shapes.

Physical conditions in larval rearing tanks are important factors for survival and growth of fish, and this is not the exception in the small-

* Corresponding author at: Graduate School of Fisheries and Environmental Sciences, Nagasaki University, 1-14 Bunkyo-machi, Nagasaki, 852-8521, Japan.
E-mail address: sakakura@nagasaki-u.ac.jp (Y. Sakakura).

https://doi.org/10.1016/j.aqrep.2020.100451
Received 24 May 2020; Received in revised form 14 August 2020; Accepted 15 August 2020
Available online 25 August 2020

scale larviculture. Many studies on larviculture had focused on physical parameters, such as water temperature (e.g., Fukuhara, 1990; Honryo et al., 2018), salinity (e.g., Bœuf and Payan, 2001) and illuminations (e.g., Villamizar et al., 2011; Stuart and Drawbridge, 2012; Honryo et al., 2018) for enhancing larval survival and growth. However, little attention has been paid to the flow field structures generated by aerators in larval rearing tanks as a factor of physical environments (Klapsis and Burley, 1984). Flow field creates upwelling and water convection in tanks that is a basic aspect for tank designs in larviculture (Harboe et al., 1998; Kolkovski et al., 2004). Previous studies (Sakakura et al., 2007, 2014, 2019) pointed out that there are species-specific optimal flow rates by aeration in rearing tanks for survival and growth of some marine fish larvae. These optimal flow rates are between stagnate (0 ml/s in aeration rates) and turbulent flow (>1000 ml/min in aeration rates). For example, the optimal flow rates for larval seven-band grouper *Epinephelus septemfasciatus* in cylindrical tanks equipped with one air stone at the center of the bottom are: 50–100 ml/min in 100-l tanks (Ruttanapornvareesakul et al., 2007), 200 ml/min for 1000-l tank, and 690 ml/min in 100-kl (m^3) tank (Sakakura et al., 2007), where the maximum flow velocity in the water column is 80 mm/s. These physical parameters expressed as actual numerical data are practically helpful for designing the rearing tanks and environments. Thus, in the process of investigating small-scale larviculture, we also aimed to quantify and visualize the flow field in the rearing tanks applied in this study.

Red seabream *Pagrus major* is an important cultured marine fish in Japan (Foscarini, 1988). Rearing techniques of red seabream had been established at the commercial scale in Japan and many studies regarding larviculture have been done with various aspects: physical parameters such as water quality (Guillén et al., 1993), water temperature and light intensity (Honryo et al., 2018), and biotic parameters such as larval development (Fukuhara, 1985; Khoa et al., 2019a, b) and nutritional requirements (e.g., Watanabe et al., 1979; Tomoda et al., 2004; Kim et al., 2014). Since this species has a long history of larviculture, we chose this species as an experimental animal, and we assumed that the development of small-scale larviculture system for *P. major* is useful not only for the experimental design of this species but also as a reference for other species. However, little attention has been paid to the small-scale larviculture experiments for this species.

In this study, we hypothesized that tank shapes and aerations may affect the survival and growth of *P. major* larvae. To test this hypothesis, we conducted larviculture experiments in small 50-l tanks of different shapes with different aeration systems. We chose a cylindrical tank (CT) with axisymmetrical flow field patterns (Sumida et al., 2013a), and a rectangular tank (RT) with three-dimensional complicated flow field patterns (Takakuwa et al., 2018), to investigate the effect of tank shapes and aerations on survival and growth of red seabream larvae. We also examined the rotifer distribution to estimate the flow field in tanks, and visualized the flow fields by simulation.

2. Materials and methods

2.1. Larviculture experiment

Three blue plastic CT (46 cm in diameter) and six blue acrylic RT (60 cm × 30 cm × 28 cm depth) containing a 50-l working volume were used in this study. The CT has aspect ratio of 1.3 (liquid depth/internal radius of the tank). We assumed that the aspect ratio of RT is also 1.3 because the water surface area and depth of RT (1.8×10^3 cm^2 ×28 cm) are almost equal to those of the CT (1.7×10^3 cm^2 × 30 cm). Artificial seawater (Marine Art Hi, Tomita Pharmaceutical, Japan) of 32 parts per thousand (ppt) was filled into each experimental tank in a 22 °C temperature-controlled room of the Aquaculture Biology Laboratory, Nagasaki University, Japan. Water flow was generated by a spherical aerator (5 cm in diameter) setting at the center on the bottom of three CTs and RTs (RT1AS) with 100 ml/min aeration rate, and two spherical aerators were placed at the bottom center of half of three RTs (RT2AS) with 50 ml/min aeration rate. We arranged the total aeration rate in each experimental tank as equal in order to make the total energy from aeration equal. Maximum light intensity at the water surface was 1000 lx with natural photoperiod.

On 20 February 2020, fertilized eggs of red seabream were purchased from a private hatchery (Ogata Suisan Co., Ltd., Kumamoto Prefecture) and were transported to the Aquaculture Biology Laboratory, Nagasaki University. Five hundred eggs were distributed into each experimental tank. Larvae were reared until 14 days post hatch (dph) with static conditions. Super Chlorella V12 (Chlorella Industry Co., Fukuoka, Japan) was added to the experimental tanks as green water, adjusting the density at 5×10^5 cells/mL once daily. Rotifers *Brachionus plicatilis* enriched with Super Chlorella V12 were fed to larvae at 10 individuals/mL when the mouth opened (3 dph). We changed 1/3 water of experimental tanks on 9 dph, but we did not remove surface substances throughout the experimental period. Water samples to assess rotifer density were collected from 9 stations (3 ml for each) in a vertical cross-section of CTs (Fig. 1a) and 27 stations in the quarter segments of RTs (Fig. 1b, c) using a pipet. Since the rotifer numbers in the experimental tanks increased during the experimental period, we standardized the rotifer distribution in the tanks each sampling day using the following equations:

$$\textit{deviation value at station } x \textit{ on day } i = (\textit{rotifer density at station } x - \textit{mean rotifer density on day } i)/\textit{standard deviation of rotifer density on day } i$$

On 14 dph, all surviving larvae in the experimental tanks were counted to calculate the survival rate. Then, 30 fish in each tank were euthanized with 200 ppm of MS222 (Tricaine; Sigma-Aldrich) and were observed under a dissecting microscope with transmitted light to see whether the swimbladder was inflated by checking air bubbles in the bladder. Then, larvae were fixed with 5 % buffered-formalin solution. Formalin-preserved fish were individually measured for morphometric characteristics by a digital microscope (VH-6300; Keyence, Osaka, Japan), and then dried at 60 °C for 24 h for measurement of the dry body weight by an ultra-micro balance (UMX2; Mettler Toledo, Columbus, OH, USA).

2.2. Flow field analysis

Two-phase bubbly flow simulations were performed in the experimental tanks using a dispersed flow model that was developed by Takakuwa et al. (2018). Its governing equations are composed of the conservation laws of mass and momentum of liquid (water) and gas (air bubble) phases, in which the effects of pressure gradient, drag and lift forces acting on bubbles, gravitational acceleration and flow viscosity are taken into account. A simplified marker and cell (SMAC) method was used to solve the governing equations. For the liquid phase, the free surface was assumed to be flat, and a no-slip boundary condition was used. On the other hand, an outflow condition was given for the gas phase at the free surface. As boundary conditions on the wall surface of tanks, a no-slip condition was given for the liquid phase, while a slip condition was given for the gas phase. An air inlet (square with a side length of 22 mm; aeration rate, 50 or 100 ml/min) was set at the center

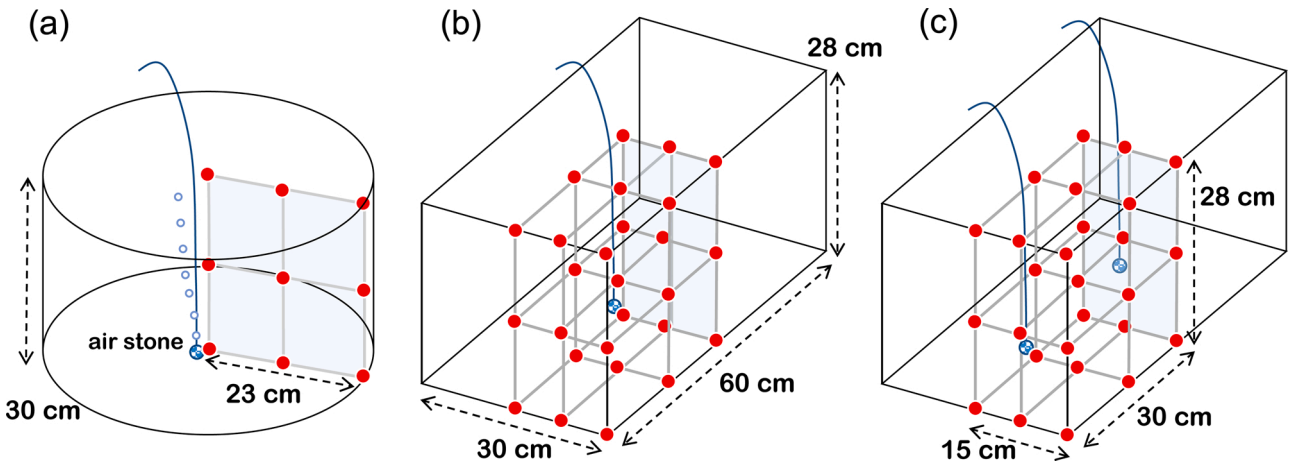

Fig. 1. Schematic drawings of the experimental tanks and aerators: (a) cylindrical tank with one air stone at the center of tank bottom, (b) rectangular tank with one air stone at the center of tank bottom and (c) rectangular tank with two air stones at the each center of half of tank bottom. Red circles are the sites where the rotifer densities were checked during the experimental period.

of the bottom surface. The diameter of a bubble was set to 2.0 mm, which is an average bubble size from the air stone used in this study and the variation of the bubble size of this air stone is reported not to affect the flow in the tank (Sumida et al., 2013b). Flow simulations were performed for 450 s, and averaged flow fields for the last 150 s are discussed in this research.

Physical environmental parameters during the experiments were as follows: water temperature 21.1–21.9 °C, salinity 32.4–32.7 ppt, dissolved oxygen 7.0–7.4 mg/l, pH 7.9, and total ammonia 0.30−0.31 mg/l.

2.3. Statistical analysis

Differences in the survival, growth and swimbladder inflation rates of larvae among tanks were determined by one-way ANOVA followed by Tukey HSD test. The rotifer distribution in tanks was standardized by the deviation value on day *i*, and were compared by one-way ANOVA followed by Tukey HSD test. All analyses were done by R 3.4.1 software, and a 5 % level of confidence was considered as a significant difference.

3. Results

3.1. Flow field in rearing tanks

Three-dimension visualization of streamlines in the experimental tanks are shown in Fig. 2. In the case of the CT, upward flows by the effect of air bubbles generated from the air stone radiated outward in the vicinity of the water surface, and then downward flows were observed along the sidewalls of the tank. In the RT1AS, the central upward flows radiated outward in the same manner as the CT, but a more complicated flow field was generated due to the effect of rectangular corners and the non-axisymmetric shape of the tank. In the RT2AS, two single-pair vortex systems forming two cubes were observed by two air stones. Cumulative areas of flow velocity magnitudes in the water column obtained from the flow simulation were shown in Fig. 3. Average flow velocity in CT was about 1.2-folds higher than those of RTs. Further, average flow velocity of total water mass (Fig. 3a) was about a half of the average flow velocity at the water surface (Fig. 3b) in every tank shape. The volume of the water with flow velocity less than 10 mm/s in total water mass in CT (40 %) is also about a half of RTs (Fig. 3). These results clearly demonstrate that the flow velocity in CT is faster than RTs, and that flow velocity is faster at the water surface in every tank. Visualization of streamlines at the surface areas are shown in Fig. 4, with color

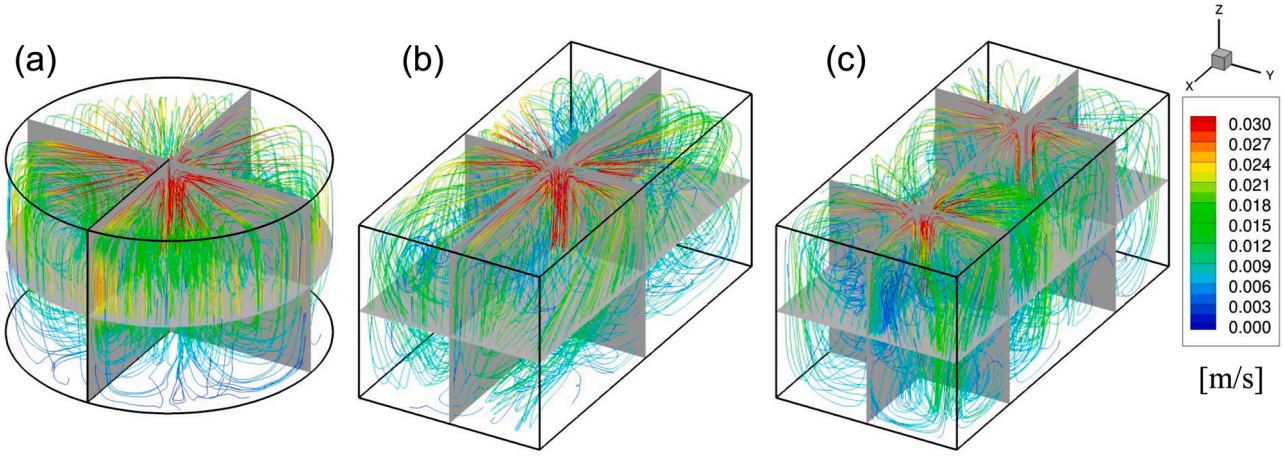

Fig. 2. Three-dimensional streamlines predicted in (a) a cylindrical tank (ø 46 × 29 cm depth) with one air stone at the bottom center with 100 ml/min aeration rate in this study, (b) a rectangular tank (60 × 30 × 28 cm depth) with one air stone at the bottom center with 100 ml/min aeration rate and (c) a rectangular tank (60 × 30 × 28 cm depth) with two air stones at the bottom center of half of tank with 50 ml/min aeration rate for each air stone.

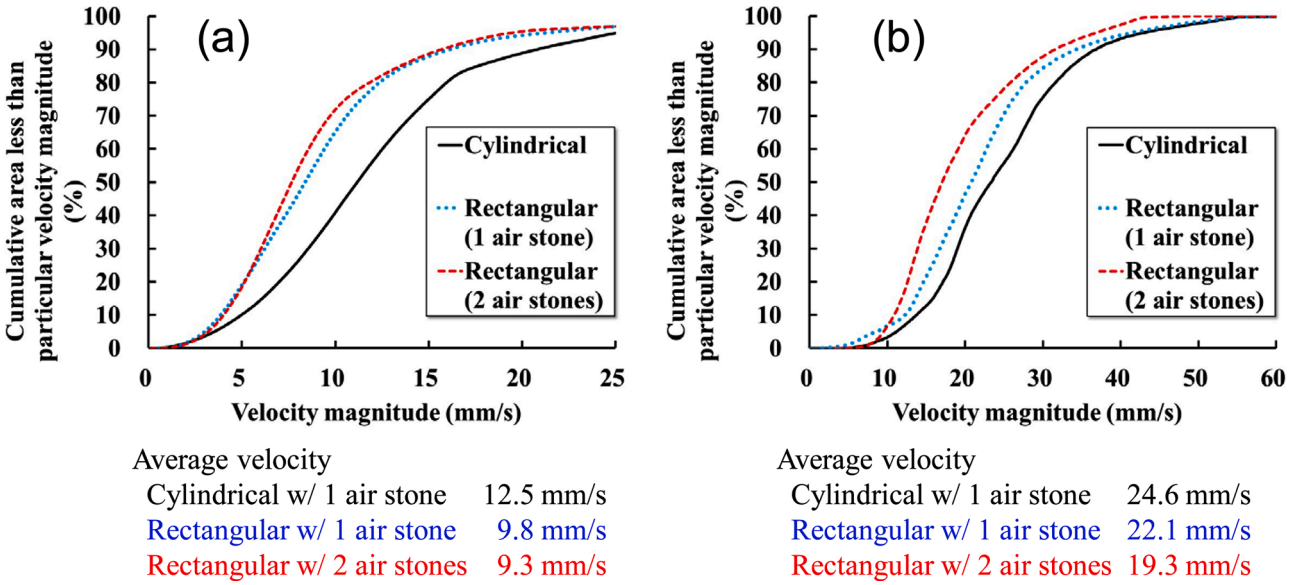

Fig. 3. Cumulative area (%) of the velocity magnitude (< *x* mm/s) (a) in total water volume and (b) at water surface, in a cylindrical tank with one air stone (CT, solid line), rectangular tanks with one air stone (RT1AS, blue dotted line) and with two air stones (RT2AS, red dotted line). For instance, (a) the water mass having a velocity between 0 and 10 mm/s occupied 40 %, 65 % and 72 % of total water volume in the CT, RT1AS and RT2AS, and (b) the water mass with a velocity between 0 and 20 mm/s occupied 36 %, 43 % and 63 % at the water surface areas in CT, RT1AS and RT2AS, respectively.

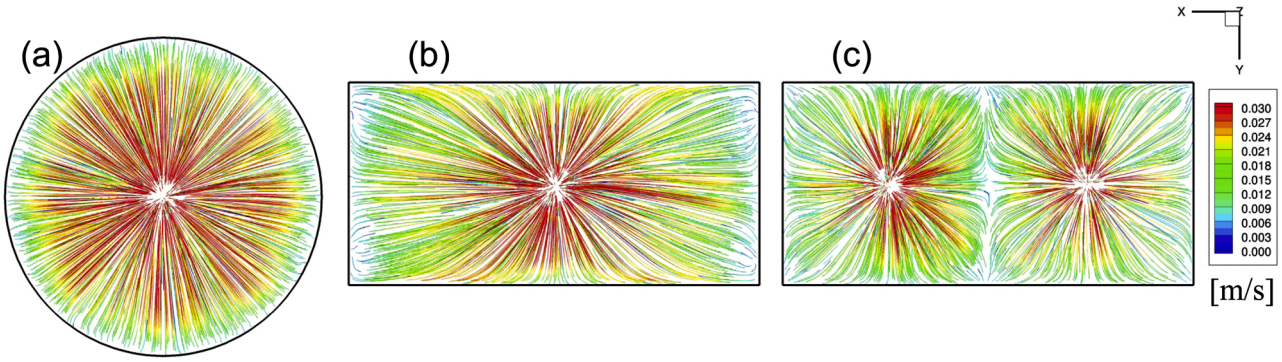

Fig. 4. Visualization of streamlines at the surface areas of (a) a cylindrical tank (ø 46 cm) with one air stone at the center of the tank, (b) rectangular tank (60 × 30 cm) with one air stone at the center of the tank, and (c) rectangular tank (60 × 30 cm) with two air stones at the center of each half of the tank.

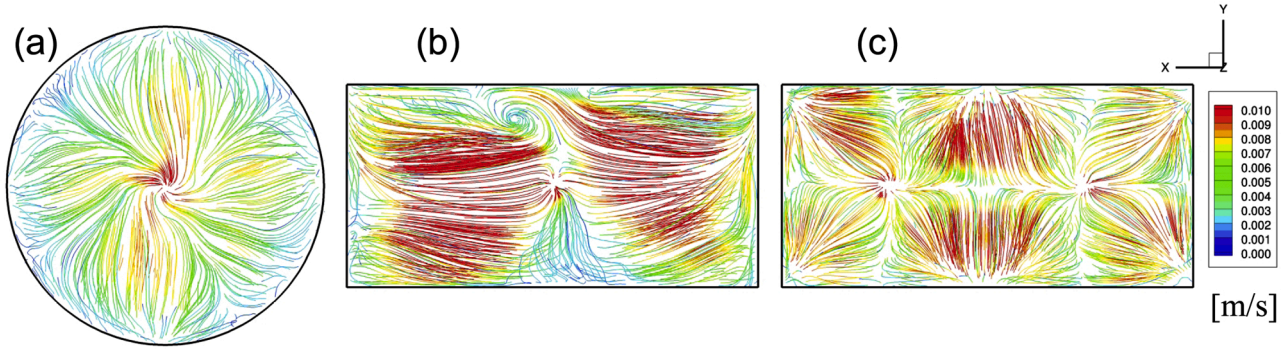

Fig. 5. Visualization of streamlines at the bottom areas of (a) a cylindrical tank (ø 46 cm) with one air stone at the center of the tank, (b) rectangular tank (60 × 30 cm) with one air stone at the center of the tank and (c) rectangular tank (60 × 30 cm) with two air stones at the center of each half of the tank.

of the flow velocity magnitude. In the CT and the RT1AS, most streamlines eventually moved toward the sidewalls of tanks and streamed as downward flows. Low velocity regions in these tanks were observed along the sidewalls of the tanks. In the RT2AS, streamlines moved toward the sidewalls and at the center of tank (between two aerators). And then, they streamed as downward flows where low velocity regions were observed. Fig. 5 shows visualization of streamlines colored by the flow velocity magnitude at the bottom areas (where water depth is more than 25 cm) in tanks. Streamlines at the bottom regions in the CT moved from the low-velocity areas along the sidewalls toward the

Table 1
Survival, growth, and swimbladder inflation rates of *Pagrus major* larvae at 14 days post hatching in different tank shapes and aerations.

Tank	Survival (%)		Growth		Swimbladder inflation (%)
			TL (mm)	BW (μg dry)	
Cylindrical	54.7 ± 11.0	^{a}	4.71 ± 0.23	165.2 ± 41.8	58.9 ± 28.3
Rectangular /w one air stone	55.3 ± 6.0	^{a}	4.94 ± 0.13	152.6 ± 38.1	94.4 ± 6.9
Rectangular w/ two air stones	29.6 ± 9.3	^{b}	4.65 ± 0.17	155.6 ± 38.1	92.2 ± 10.7

Abbreviation: TL=total length, BW=body weight. Results are mean values ± SD (n=3). Alphabets in superscripts in the column represent significant differences (a>b, Tukey HSD test, p<0.05: see details in Table 2).

air stone, where they reverted to the upward flows. Streamlines from both short sides of the rectangle created a vortex in RT1AS, colliding in the vicinity of the center of the long sides. Low velocity regions were observed along the sidewalls in the RT1AS and the RT2AS but they were also found from the aerator to tank walls in the RT2AS and between the two aerators. Streamlines toward the air stones in the RT2AS did not form a vortex like in RT1AS. Flow structures were more complicated in both the RT1AS and RT2AS than in the CT, and low flow velocity magnitude at the bottom regions were larger contrary to the surface area.

3.2. Rotifer distribution

Rotifer density increased throughout the experimental period, reaching 49.9 individuals/mL in CT, 60.5 individuals/mL in RT1AS and 82.2 individuals/mL in RT2AS at 14 dph, respectively (n = 6). Rotifer distribution expressed as an average of deviation values was significantly higher at the edge of the tank wall in CT (one-way ANOVA, $n = 6$, $df = 8$, $F = 38.31$, $p = 2.0\times e^{-16}$; Tukey HSD, $p < 0.05$), from the air stone to the tank walls in RT1AS (one-way ANOVA, $n = 6$, $df = 26$, $F = 11.43$, $p = 2.0\times e^{-16}$; Tukey HSD, $p < 0.05$), and between two air stones in RT2AS (one-way ANOVA, $n = 6$, $df = 26$, $F = 6.382$, $p = 1.6\times e^{-16}$; Tukey HSD, $p < 0.05$; Fig. 6).

3.3. Survival, growth and swimbladder inflation rates of larvae

The hatching rate of eggs was 98.3 ± 2.9 %. When we sampled 10 fish from each tank on 4 dph, one day after the mouth opening, we recognized rotifers in all larval guts. The survival rates at 14 dph in CT (54.7 ± 11.0 %) and RT1AS (55.3 ± 6.0 %) were significantly higher than RT2AS (29.6 ± 9.3 %, $p < 0.05$, Tukey HSD test; Tables 1, 3). The body length and dry weight of larvae at 14 dph were not significantly different among tanks (Tables 1, 3). Swimbladder inflation rates were also not significantly different between tank shapes and aerators (Tables 1, 3), but CT (58.9 ± 28.3 %) showed lower trend than RTs (80–100 %). We could not detect any external deformities during the observation for swimbladder inflation. Morphological parameters and their proportions were not significantly different between tank shapes and aerations, either (Tables 2, 3).

4. Discussion

Survival rate of red seabream larvae in CT and RT1AS at 14 dph was almost two-folds higher than that in RT2AS. The survival rate of red seabream in CT was comparable to that of Pacific bluefin tuna *Thunnus orientalis* larvae at 8 dph in the same CT (52.7 %; Aung Naing Win et al., 2020), whereas survival in the RT1AS was different between red seabream (55.3 %) and bluefin tuna (0.8 %). The different survival rates between red seabream and Pacific bluefin tuna in RT1AS is presumably due to the occurrence of sinking syndrome in larval bluefin tuna, where

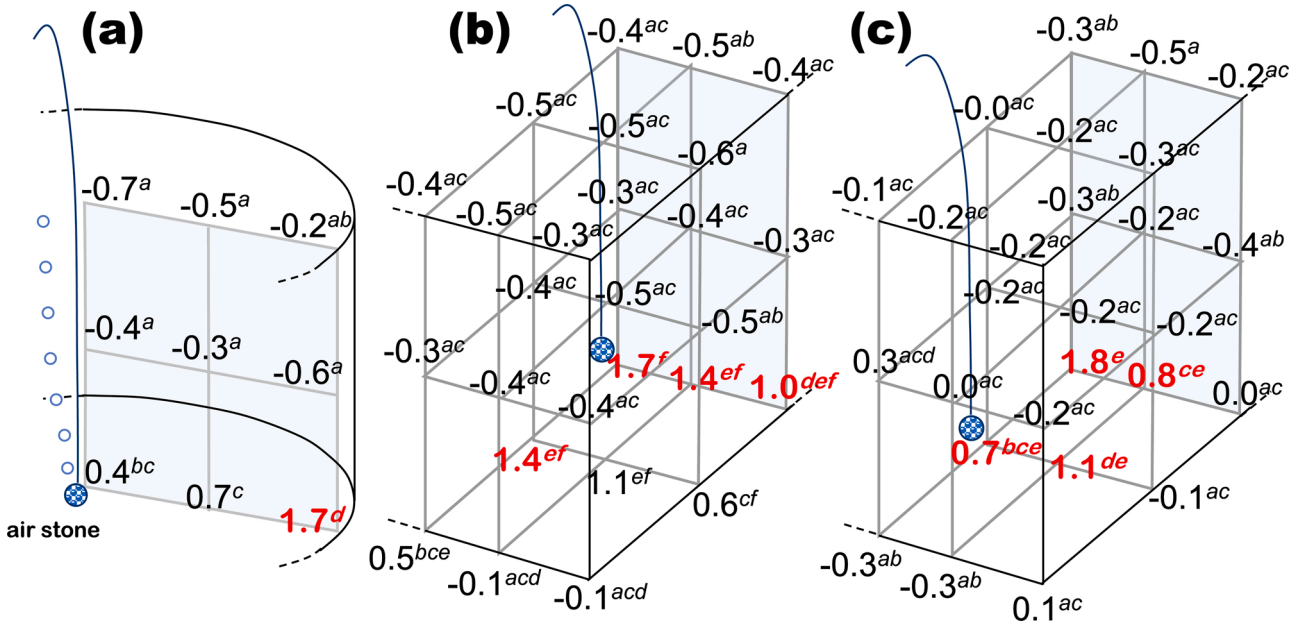

Fig. 6. Rotifer distribution (a) at half cross section in cylindrical tank, (b) and (c) in the quadrisection in a rectangular tanks. Values are average of deviation values during culture period (n = 6, a < b<c < d<e < f, Tukey HSD, $p < 0.05$).

Table 2
Morphological parameters of *Pagrus major* larvae at 14 days post hatching in different tank shapes and aerations.

Tank	Morphological parameter (mm)				proportion			
	SL	BD	HL	ED	BD/SL	HL/SL	ED/SL	ED/HL
Cylindrical	4.51 ± 0.25	1.11 ± 0.08	1.22 ± 0.06	0.46 ± 0.01	0.247 ± 0.013	0.270 ± 0.009	0.102 ± 0.005	0.378 ± 0.009
Rectangular /w one air stone	4.76 ± 0.12	1.10 ± 0.08	1.22 ± 0.10	0.48 ± 0.03	0.231 ± 0.012	0.256 ± 0.014	0.100 ± 0.005	0.394 ± 0.004
Rectangular w/ two air stones	4.45 ± 0.18	1.05 ± 0.09	1.18 ± 0.07	0.45 ± 0.02	0.235 ± 0.013	0.265 ± 0.012	0.102 ± 0.002	0.388 ± 0.010

Results are mean values ± SD ($n = 3$). Abbreviation: SL = standard length, BD = body depth, HL = head length, ED = eye diameter.

Table 3
Results of one-way ANOVA for the effect of tank shape and aeration on the survival, growth and swim bladder inflation of *Pagrus major* larvae at 14 days post hatching ($n = 3$).

Parameters		*df*	Mean squares	*F*	*p*-value
Survival		2	0.08047	7.537	0.0231
Swimbladder inflation		2	0.3914	3.767	0.0871
Growth	BW	2	129.3	0.083	0.921
	TL	2	0.07148	2.141	0.199
	SL	2	0.08110	2.300	0.181
	BD	2	0.003733	0.555	0.601
	HL	2	0.002033	0.329	0.732
	ED	2	0.000433	1.026	0.414
Proportion	BD/SL	2	0.000183	1.172	0.372
	HL/SL	2	0.000149	1.089	0.395
	ED/SL	2	0.000003	0.177	0.842
	ED/HL	2	0.000175	2.524	0.160

Abbreviation: TL = total length, SL = standard length, BD = body depth, HL = head length, ED = eye diameter.

T. orientalis larvae with higher body density sink to the bottom of the tank during dark periods due to low swimming activity and cause mortality at the bottom of the rearing tank (Takashi et al., 2006; Tanaka et al., 2009). Sinking bluefin tuna larvae were assumed to be trapped into low flow areas at the bottom of RT1AS (Win et al., 2020). On the contrary, sinking syndrome is not observed in larval red seabream, and thus, similar survivals were observed between CT and RT1AS.

Survival rate of red seabream in RT2AS (29.6 %) was low in this study. In the CT and RT1AS, a single-pair vortex system could be observed at the central sections. Low velocity regions in these tanks were observed along the sidewalls of the tanks and bottom areas. These low-flow areas were coincided with higher density of rotifer distribution at the bottom (Fig. 6a, b), but these areas are smaller in the CT than in the RT1AS (Win et al., 2020). In the RT2AS, two-vortex systems were formed between two aerators. The bubbles from two air stones may stun fish larvae more frequently and had larvae contacting the tank walls and bubbles than one air stone. Thus, we presume that the survival of red seabream larvae in RT2AS was lower than that in RT1AS and CT.

Growth and swimbladder inflation of red seabream larvae at 14 dph were not significantly different between different tank shapes with different aeration systems. It is similar to the previous findings, in which tank shapes affected larval survival but not growth of seven-band grouper *Epinephelus septemfasciatus*, devil stinger *Inimicus japonicus* (Ruttanapornvareesakul et al., 2007) and Pacific bluefin tuna (Aung Naing Win et al., 2020). However, swimbladder inflation rate in the CT was slightly lower and varied rather than the RTs. Swimbladder inflation of marine fish larvae is initiated by gaping air from the water surface and introducing it into swimbladder through the pneumatic duct after mouth opened (Kitajima et al., 1981). With the respect of water surface in tanks of the present study, streamlines radiated from air stone were straight forward to the side walls in CT and RT1AS, and straight forward to the side walls and to the middle of tanks in RT2AS (Fig. 4). Flow velocity in CT was around 1.2 times higher than these in RT1AS and RT2AS (Fig. 3). Since the average swimming speed of larval red seabream is reported as 1 standard length/s (Fukuhara, 1985), we can estimate the swimming speed of red seabream larvae in this study was less than 4.6 mm/s (Table 2). The water mass with the flow velocity less than 4.6 mm/s was 8.6 % in CT whereas it was almost 2-folds in CTs (15.3–15.9 %, Fig. 3a). High water velocity at surface area in CT may prevent the larvae not only from attaching to water surface (Sakakura et al., 2019), but also gaping air through the water surface that will lead to failure of swim-bladder inflation.

Failure of swim bladder inflation in the larval phase is known to cause malformations such as saddleback and scoliosis that will occur when the fish reached juvenile phase (Kitajima et al., 1981). It is noteworthy that high swim bladder inflation rates were observed without any external deformity of larval *P. major* in this study, although we did not remove surface substrates. However, this may be because the larvae in this study (SL < 5.0 mm) were too small to detect malformations, where fish did not reach the notochord-flexion phase (SL > 5.6 mm) and their vertebrate were not ossified (Fukuhara, 1985). It is possible that some fish in cylindrical tank with low swim bladder inflation rate (30 % in the one tank of CT) may show the scoliosis when they reached juvenile phase (SL > 7.6 mm: Fukuhara, 1985). Thus, further detailed studies are required to elucidate the influence of flow field on swimbladder inflation and analysis of allometry (Réalis-Doyelle et al., 2018) to detect malformations in *P. major* larvae and juveniles.

In conclusion, flow fields in different tank shapes and aerations affected the survival of red seabream larvae. Flow field created by a single air stone in small-scale 50-l tanks was a preferable for red seabream larvae, but swimbladder inflation may be different by tank shapes. We can recommend 50-l rectangular tank with one air stone system for red seabream larvae because of the relatively high and stable survival and swim bladder inflation rate. We also propose that measuring live feed densities at the various points of larviculture tank is practical method for estimating the flow velocity in a tank, especially for finding a stagnate area where high density of live feed can be detected.

CRediT authorship contribution statement

Writing - original draft, Investigation, Data curation. **Wataru Yamazaki:** Formal analysis. **Tetsuya Sumida:** Formal analysis. **Atsushi Hagiwara:** Supervision, Funding acquisition. **Yoshitaka Sakakura:** Supervision, Writing - review & editing, Funding acquisition.

Declaration of Competing Interest

The authors report no declarations of interest.

Acknowledgements

The first author is grateful to The Ministry of Education, Culture, Sports, Science and Technology of Japanese Government (Monbukagakusho Scholarships program) for the financial aid. This study was financially supported by a Grant-in-Aid for Scientific Research (19K22338, 20H03063), Japan Society for the Promotion for Science.

References

Bœuf, G., Payan, P., 2001. How should salinity influence fish growth? Comp. Biochem. Physiol. – C Toxicol. Pharmacol. 130, 411–423. https://doi.org/10.1016/S1532-0456(01)00268-X.

Cook, M.A., Massee, K.C., Wade, T.H., Oden, S.M., Jensen, C., Jasonowicz, A., Immerman, D.A., Goetz, F.W., 2015. Culture of sablefish (*Anoplopoma fimbria*) larvae in four experimental tank designs. Aquac. Eng. 69, 43–49. https://doi.org/10.1016/j.aquaeng.2015.09.003.

Estudillo, C.B., Duray, M.N., Marasigan, E.T., 1998. Growth and survival of milkfish (*Chanos chanos*), seabass (*Lates calcarifer*) and rabbitfish (*Siganus guttatus*) larvae reared at the same density in different sized tanks. Isr. J. Aquac. – Bamidgeh 50, 20–24.

Foscarini, R., 1988. A review: intensive farming procedure for red sea bream *(Pagrus major)* in Japan. Aquaculture 72, 191–246. https://doi.org/10.1016/0044-8486(88)90212-8.

Fukuhara, O., 1985. Functional morphology and behavior of early life stages of red sea bream. Bull. Jpn. Soc. Sci. Fish. 51 (5), 731–743. https://doi.org/10.2331/suisan.51.731.

Fukuhara, O., 1990. Effects of temperature on yolk utilization and initial growth, and behavior of unfed marine fish-larvae. Mar. Biol. 106, 169–174. https://doi.org/10.1007/BF01314797.

Guillén, J.L., Endo, M., Turnbull, J.F., Kawatsu, H., Richards, R.H., Aoki, T., 1993. Depressed growth rate and damage to the cartilage of red sea bream larvae associated with exposure to ammonia. Nippon. Suisan Gakkaishi 59 (7), 1231–1234. https://doi.org/10.2331/suisan.59.1231.

Harboe, T., Mangor-gensen, A., Naas, K.E., Næss, T., 1998. A tank design for first feeding of Atlantic halibut, *Hippoglossus hippoglossus* L., larvae. Aquac. Res. 29, 919–923. https://doi.org/10.1046/j.1365-2109.1998.29120919.x.

Honryo, T., Kurata, M., Sandval, D., Yamao, S., Cano, A., Sawada, Y., 2018. Effect of water temperature and light intensity on swim bladder inflation and growth of red sea bream *Pagrus major* larvae. Fish. Sci. https://doi.org/10.1007/s12562-018-1194-5.

Houde, E.D., 1972. Some recent advances and unsolved problems in the culture of marine fish larvae. Proc. Annu. Work. – World Maric. Soc. 3, 83–112. https://doi.org/10.1111/j.1749-7345.1972.tb00050.x.

Khoa, T.N.D., Waqalevu, V., Honda, A., Shiozaki, K., Kotani, T., 2019a. Early ontogenetic development, digestive enzymatic activity and gene expression in red sea bream (*Pagrus major*). Aquaculture 512. https://doi.org/10.1016/j.aquaculture.2019.734283, 734–283.

Khoa, T.N.D., Waqalevu, V., Honda, A., Shiozaki, K., Kotani, T., 2019b. Comparative study on early digestive enzyme activity and expression in red sea bream (*Pagrus major*) fed on live feed and micro-diet. Aquaculture 519. https://doi.org/10.1016/j.aquaculture.2019.734721.

Kim, H.J., Sakakura, Y., Maruyama, I., Nakamura, T., Takiyama, K., Fujiki, H., Hagiwara, A., 2014. Feeding effect of selenium enriched rotifers on larval growth and development in red sea bream *Pagrus major*. Aquaculture 432, 273–277. https://doi.org/10.1016/j.aquaculture.2014.05.021.

Kitajima, C., Tsukashima, Y., Fujita, S., Watanabe, T., Yone, Y., 1981. Relationship between uninflated swim bladder and lordotoic deformity in hatchery-reared red sea bream *Pagrus major*. Bull. Jpn. Soc. Sci. Fish. 47 (10), 1289–1294. https://doi.org/10.2331/suisan.47.1289 (in Japanese with English abstract).

Klapsis, A., Burley, R., 1984. Flow distribution studies in fish rearing tanks. Part 1-design constraints. Aquac. Eng. 3, 103–118. https://doi.org/10.1016/0144-8609(84)90002-5.

Kolkovski, S., Curnow, J., King, J., 2004. Intensive rearing system for fish larvae research: I. Marine fish larval rearing system. Aquac. Eng. 31, 295–308. https://doi.org/10.1016/j.aquaeng.2004.05.004.

Moodie, G.E.E., Mathias, J.A., Loadman, N.L., 1992. A comparison of two production-scale modules for the intensive culture of larval walleye. Aquac. Eng. 11, 171–182. https://doi.org/10.1016/0144-8609(92)90003-G.

Moore, A., Prange, M.A., Summerfelt, R.C., Bushman, R.P., 1994. Evaluation of tank shape and a surface spray for intensive culture of larval walleyes fed formulated feed. Progress. Fish-Culturist 56, 100–110. https://doi.org/10.1577/1548-8640(1994)056<0100:EOTSAA>2.3.CO;2.

Moorhead, J.A., 2015. Research-scale tank designs for the larval culture of marine ornamental species, with emphasis on fish. Aquac. Eng. 64, 32–41. https://doi.org/10.1016/j.aquaeng.2014.11.004.

Réalis-Doyelle, E., Gisbert, E., Alcaraz, C., Teletchea, F., Pasquet, A., 2018. Temperature affects growth allometry and development patterns in brown trout (*Salmo trutta*) fry: a multitrait approach. Can. J. Fish. Aquat. Sci. 75, 714–722. https://doi.org/10.1139/cjfas-2017-0037.

Ruttanapornvareesakul, Y., Sakakura, Y., Hagiwara, A., 2007. Effect of tank proportions on survival of seven-band grouper *Epinephelus septemfasciatus* (Thunberg) and devil stinger *Inimicus japonicus* (Cuvier) larvae. Aquac. Res. 38, 193–200. https://doi.org/10.1111/j.1365-2109.2007.01653.x.

Sakakura, Y., Shiotani, S., Chuda, H., Hagiwara, A., 2007. Flow field control for larviculture of the seven-band grouper *Epinephelus septemfasciatus*. Aquaculture 268, 209–215. https://doi.org/10.1016/j.aquaculture.2007.04.042.

Sakakura, Y., Andou, Y., Tomioka, C., Yogo, S., Kadomura, K., Miyaki, K., Hagiwara, A., 2014. Effects of aeration rate and salinity gradient on the survival and growth in the early life stages of the devil stinger *Inimicus japonicus*. Aquac. Sci. 62 (1), 99–105. https://doi.org/10.11233/aquaculturesci.62.99.

Sakakura, Y., Yamazaki, W., Takakuwa, Y., Sumida, T., Takebe, T., Hagiwara, A., 2019. Flow field control in marine fish larviculture tanks: lessons from groupers and bluefin tuna in Japan. Aquaculture 498, 513–521. https://doi.org/10.1016/j.aquaculture.2018.09.012.

Stuart, K.R., Drawbridge, M., 2012. The effect of photoperiod on larval culture performance of two marine finfish species. Aquaculture 360–361, 54–57. https://doi.org/10.1016/j.aquaculture.2012.07.017.

Sumida, T., Kawahara, H., Shiotani, S., Sakakura, Y., Hagiwara, A., 2013a. Observations of flow patterns in a model of a marine fish larvae rearing tank. Aquac. Eng. 57, 24–31. https://doi.org/10.1016/j.aquaeng.2013.06.002.

Sumida, T., Kawahara, H., Shiotani, S., Sakakura, Y., Hagiwara, A., Yamamoto, K., 2013b. Numerical calculation of flow field in a model of rearing tank for marine fish larvae. J. Fish. Eng. 49, 155–165. https://doi.org/10.18903/fisheng.49.3_155.

Takakuwa, Y., Yamazaki, W., Sumida, T., Sakakura, Y., 2018. Flow field investigation in rectangular tanks by bubbly flow simulations. Fish. Eng. 54, 155–162. https://doi.org/10.18903/fisheng.54.3_155 (in Japanese with English abstract).

Takashi, T., Kohno, H., Sakamoto, W., Miyashita, S., Murata, O., Sawada, Y., 2006. Diel and ontogenetic body density change in Pacific bluefin tuna, *Thunnus orientalis* (Temminck and Schlegel), larvae. Aquac. Res. 37, 1172–1179. https://doi.org/10.1111/j.1365-2109.2006.01544.x.

Tanaka, Y., Kumon, K., Nishi, A., Nikaido, H., Eba, T., Shiozawa, S., 2009. Status of the sinking of hatchery-reared larval Pacific bluefin tuna on the bottom of the mass culture tank with different aeration design. Aquac. Sci. 57, 587–593. https://doi.org/10.11233/aquaculturesci.57.587.

Theilacker, G.H., 1980. Rearing container size affects morphology and nutritional condition of larval jack mackerel, *Trachurus symmetricus*. Fish. Bull. 78, 789–791.

Tomoda, T., Koiso, M., Kuwada, H., Chern, J.-N., Takeuchi, T., 2004. Dietary value of marine rotifer Brachionus plicatilis in different population growth stages for larval red seabream *Pagrus major*. Nippon. Suisan Gakkaishi 70, 573–582. https://doi.org/10.2331/suisan.70.573.

Tucker, J.W., 1998. The rearing environment. In: Tucker, J.W. (Ed.), Marine Fish Culture. Kluwer Academic Publishers, London, pp. 49–148.

Villamizar, N., Blanco-Vives, B., Migaud, H., Davie, A., Carboni, S., Sánchez-Vázquez, F. J., 2011. Effects of light during early larval development of some aquacultured teleosts: a review. Aquaculture 315, 86–94. https://doi.org/10.1016/j.aquaculture.2010.10.036.

Watanabe, T., Oowa, F., Kitajima, C., Fujita, S., Yone, Y., 1979. Relationship between the dietary value of rotifers *Brachionus plicatilis* and their content of ω3 highly unsaturated fatty acids. Nippon. Suisan Gakkaishi 45, 883–889. https://doi.org/10.2331/suisan.45.883.

Win, Aung Naing, Yamazaki, W., Hasegawa, T., Higuchi, K., Takashi, T., Gen, K., Sumida, T., Hagiwara, A., Sakakura, Y., 2020. Effect of tank shape on survival and growth of Pacific bluefin tuna *Thunnus orientalis* larvae. Aquaculture 524. https://doi.org/10.1016/j.aquaculture.2020.735283.